Iran University of Science and Technology

International Journal of

Railway Research

ISSN: 2423-3838

Assessment of collision-induced derailment of single wheelset on curved tracks by rail removing and lateral impact

Alireza Kardanian[1], Parisa Hosseini Tehrani[1*]

[1]School of Railway Engineering, Iran University of Science and Technology, Iran, Tehran.

ARTICLE INFO

Article history:
Received: 22.06.2022
Accepted: 10.01.2023
Published: 22.01.2023

Keywords
derailment
curve
wheelset
impact
rail

A B S T R A C T

Significant lateral and vertical impact forces can cause a derailment on the curved tracks. In this work, we try to indicate the similarities and differences between derailment modes on the curved track due to the lateral impact, considering the position and importance of the impact force itself and the rail removal. The obtained results may be used to design the passive safety systems. A wheelset with six degrees of freedom is considered, and the impact force is applied as a step function for both considered scenarios. In a curve with a large radius (above 4000 meters), the derailment modes become similar to the straight track. In the smaller radius curves, it is seen that the anti-clockwise derailment is more likely. But this derailment process takes more time in comparison with the clockwise (toward the center of the curves) derailment. The higher velocity of the wheelset leads to a shorter derailment time. In the case of the rail removal, velocity above 50 m/s affects the derailment significantly, and removing the outer rail in the curved track cause derailment while removing the inner rail will not cause derailment under any circumstances.

1. Introduction and background

Every year, derailments caused by different reasons lead to catastrophic casualties. Forced vibrations and collisions usually are involved in rail vehicle derailment [16,19]. Most of the train models take the coupled rail-vehicle dynamics into account for derailment analysis.

Wheel-rail contact condition and relative wheel displacement concerning the initial condition are specific criteria for checking derailment. The derailment may have several causes, such as collision and dynamic instabilities of the rail vehicles, rail defects, irregularities, and earthquakes.

The main focus of this paper is collision-induced derailment considering the following two scenarios. The first one evaluates the performance of a wheelset under lateral impact force, and the second one considers the derailment of the wheelset due to the removal of the rail.

The first type of derailment was due to the crash of a rail vehicle. The second type occurs due to the rail removal from the track, where the wheelset falls and a significant vertical impact force will be applied to the wheelset. Figure 1 shows a derailed train due to rail removal (in Iran 2020). The massive damages which are occurred may be considered. This event is usually rare, but it seems that not much research has been done on derailment due to rail removal.

In this regard, Pater [1] proposed an analytic wheelset model on the curved track with constant curve radius and superelevation (Cant). In his work, to reduce the complexity of the

*Corresponding author
Email address: hosseini_t@iust.ac.ir

[DOI: 10.22068/ijrare.306]

contact theory, all displacements were considered small. Wheel-rail contact with different friction coefficients on curved tracks was studied by Iwincki [2]. A random energy theory was developed to evaluate the derailment of a freight train, considering derailment geometric criterion and train track transverse vibration analysis and other parameters, by Xiang et al. [3].

Sweet et al. [4] evaluated wheelset derailment under lateral impact with steady rolling and presented the results relating to cases with variable forces and moments. A virtual testing model used for high-speed Korean trains for design and collision safety goals, factors which affect passenger safety, including buckling, zigzagging, chain reaction, and overriding of a train, identified by Kim et al. [5]. A theoretical model for a single wheelset that undergoes lateral impact was evaluated and different types of the derailment were specified by Koo et al. [6]. Torstensson et al. [7] studied the low-frequency and high-frequency dynamics of vehicle-track interaction on the small radius curves. They examined several parameters, such as wheelset and rail flexibility, inertial forces, and centrifugal forces. They showed that eigenmodes are very important and affect the creep forces. A theoretical model for a single wheelset was developed by Koo et al. [8] for the prediction of wheelset derailment, considering the vertical and horizontal impact forces on the wheelset. The derailment of a city tram by a multi-body dynamics approach associated with a crash absorber was investigated by Zhao et al. [9]. A flexible railroad axle was assessed for wheel-rail contact on curved tracks by Cases et al. [10]. A theoretical model for a single wheelset was obtained to predict the derailment coefficient under different circumstances by Koo et al. [11]. Braking on curved tracks with a multi-body dynamics approach was investigated to identify wheel-rail contact by Liu et al. [12]. The three-dimensional multibody dynamic formulation is used to model the derailment of a train due to heavy truck impact, by Ling et al [13], their model predicts wheel-climb derailment and overturning. The frontal collision derailment of the multi-body system at the level crossing examined by Ling et al. [14], Considering a complex coupled dynamic model using a FASTSIM algorithm for wheel-rail contact.

Ling et al. applied a model to investigate the collision-induced derailment on the curved tracks [15]. Ling et al. [16], showed by using the guardrails, the risk of derailment due to the collision at the level crossing was reduced. Ling et al. [17] utilized the coupled finite-element and multi-body dynamics model of a freight train. Their founding indicated that an increase in yaw angle is a sign of instability. In Yao et al. [18], a nonlinear finite element method was used to analyze the collision-induced derailment of subway train vehicles, wheelset relative displacement, and rotation of couplings of the first wagon were considered primary signs of derailment. A train-track-bridge model was taken into account to assess collision-induced derailment on the bridge by Ling [19]. Yao et al. [20] evaluated the mechanism of derailment of subway trains due to oblique collision by finite

Figure 1. Derailment of the train due to rail removing (Iran 2020)

[DOI: 10.22068/ijrare.306]

element modeling. Their results indicate that the angle of impact mostly affects the pattern of derailment. Recently, the development of energy-absorbing structures for a railway vehicle to minimize injuries and a self-protective posture for occupants is studied by Gao et al. [21]. Choi et al. [22] Investigated the effect of rail roughness on high-speed train movement and found that track alignment has a greater effect on train operational safety. Cheng et al. [23] considered the effect of rail roughness and earthquake on a tilted rail vehicle in curves. They showed the simultaneous effects of these two phenomena. Dyk et al. [24] evaluated the impact wheel load factor for more realistic loading conditions and better designs. Cheng et al. [25] considered the tilting train with wind and earthquake loads and rail roughness. They also used nonlinear creep theory in the modeling and found that each mode of rail roughness has its special effects on the coefficient of derailment.

In most previous studies, the goal was to understand the derailment phenomena under different circumstances, including collision-induced derailment. However, the position of the derailing impact force and nature of collision-induced derailment under different circumstances, especially on curved tracks, should be analyzed exactly for designing energy-absorbing and protective structures in railway vehicles.

In this task, we try to indicate the similarities and differences between derailment modes on the curved track due to lateral impact and rail removal. The obtained results may guide improving the passive safety of a railcar considering different derailment scenarios. The position and importance of the impact force itself may assist us in designing suitable energy absorbers for a rail vehicle system.

The rail wheelset interaction was not fully analyzed, considering the wheelset falling off due to lack of the rail. However, it is a case of derailment and may cause significant damage to passengers and rail vehicles. In this regard, another goal of this paper is to analyze the wheelset performance after falling. Finally, a comparison between two considered derailment scenarios is performed, and suggestions for reducing the damage are presented.

2. Methods and Modelling

The curving effect determines the difference between the derailment response of a wheelset. In this work, a simple wheelset model is used to investigate derailment on the curved tracks. SIMPACK package is used for derailment analysis. The constructed model has six degrees of freedom. The model characteristics are as follows.

The Standard rail gauge (1435 mm) according to UIC 60 adopted and the wheelset belongs to a high-speed rail vehicle. The wheel diameter and profile are 920 mm, and S1002 respectively. The dead loads with the magnitude of 82 kN are applied at the ends of the axle (WL and WR). Impact load (F) is perpendicular to the vertical axle and parallel to the wheel axle (Figure 2 (c)).

2.1. Evaluation of simulation

For verification of modeling, the derailment coefficient of the current wheelset model is compared to the result of reference [11]. The derailment coefficient is defined as follows

$$c = \frac{Q}{P} = \frac{lateral\ wheel\ force}{Vertical\ wheel\ force} \qquad (1)$$

Koo et al. [11] proposed a theoretical derailment coefficient for wheel climbing and wheel lifting condition based on a free diagram of the wheelset and with which we compare the derailment coefficients of current work, the equations related to the derailment coefficient for wheel climbing derailment is

$$\frac{Q}{P} = \frac{R_F coa\alpha - uR_F sin\alpha + \mu\, R_R}{R_F sin\alpha + uR_F cos\alpha + \mu\, R_R} \qquad (2)$$

where RF, RR, and α are illustrated in Figure 2 (c), μ is the friction coefficient, and derailment coefficient for lift up condition is as follows

$$\frac{Q}{P} = \frac{R_F coa\alpha + uR_F sin\alpha + \mu\, R_R}{R_F sin\alpha - uR_F cos\alpha + \mu\, R_R} \qquad (3)$$

According to Figure (2c) WR, WL, and F are loads of right and left wheel and lateral impact force, respectively.

In Figures 3 (a), and 3 (b) the loading history for rollover, and climb-up conditions for a single wheelset are illustrated. As seen, the left and the right wheel loads remain constant, but the impact lateral force changes linearly. In Figure 3 (c), the derailment coefficients are shown at the derailment moment for the climb-up and the

[DOI: 10.22068/ijrare.306]

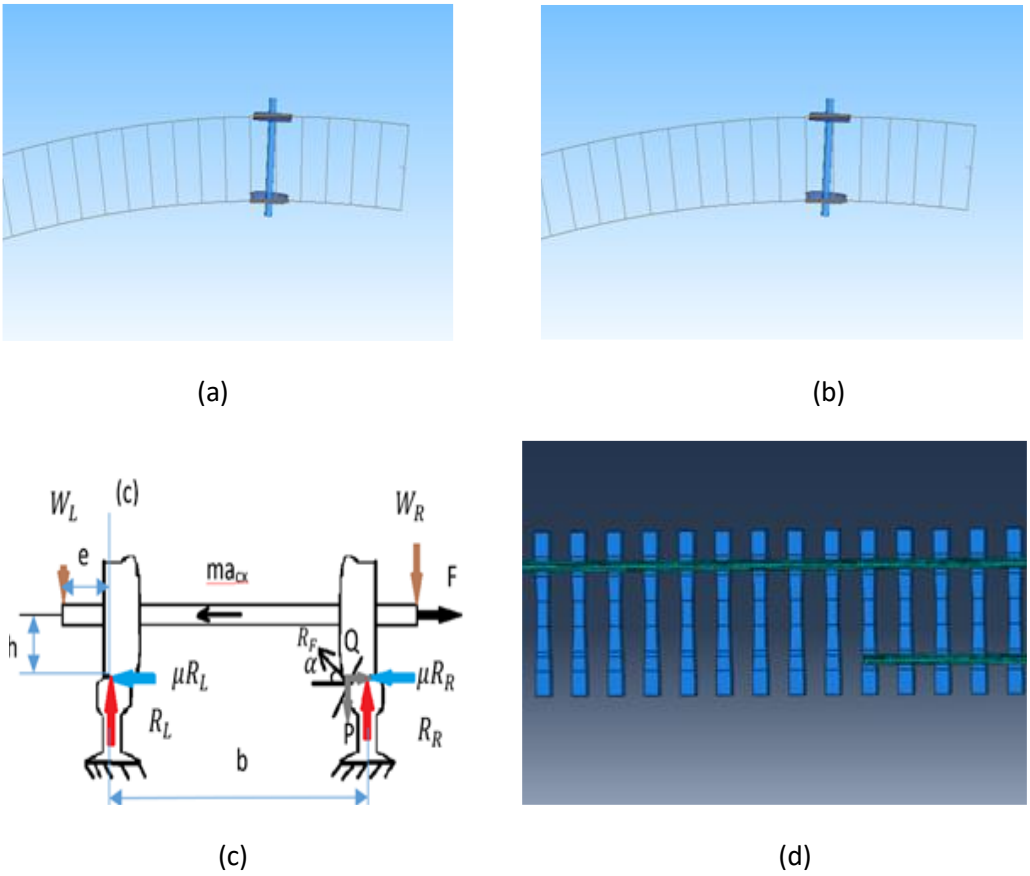

Figure 2. (a) Lateral impact force toward the center of curve (Clockwise derailment). (b) Lateral impact force toward the outside of curve (Anti-clockwise derailment). (c) Wheelset Free body diagram. (d) Rail removal formation

rollover conditions (Picked with arrows). For verification, the results of the current work are compared with the results of Koo et al. [11] in Table 1. All data relating to this comparison are directly taken from [11].

2.2. Wheelset model on the curved tracks (Lateral impact due to external force)

To provide collision-induced derailment, lateral impact load is applied as a step function at the midpoint of the time interval (100 milliseconds from the beginning). The FASTSIM algorithm is used to calculate wheel-rail contact and creep forces at the wheel-rail interface. The friction coefficient is considered 0.3 for all models. There are two derailment modes on the curved track. The first derailment mode happens when the lateral impact force is toward the center of the curve which can be seen in Figure 2(a) (clockwise derailment mode). The second mode is when the direction of the lateral impact force is toward the outer rail according to Figure 2(b) (anti-clockwise derailment mode). We analyzed the wheelset on the straight track to obtain a derailment coefficient of C. For the curved tracks, small radiuses are 100, 200, and 400 meters, and the large ones are 4000 and 8000 meters. Considered superelevations (cant) for the curved track are 0 and 0.15 of a meter. Clockwise and anti-clockwise derailment are both studied on the curved track. On the curve, wheelset conditions will change due to the inertial forces of the wheelset. For all considered wheelset models, a 300kN lateral force is applied, which can cause derailment under any circumstance. By considering force as a constant variable, other influencing variables can change and their effects on the derailment modes can be observed. In this part, obtaining the derailing impact force is not our desire. During the investigation of the derailment modes on the curve, changes in velocity (10, 25, 50, 75, and 90 m/s), curve radii, and superelevation are considered. In Figure 4 (a) loading history for a wheelset negotiating an arbitrary radius curve is

[DOI: 10.22068/ijrare.306]

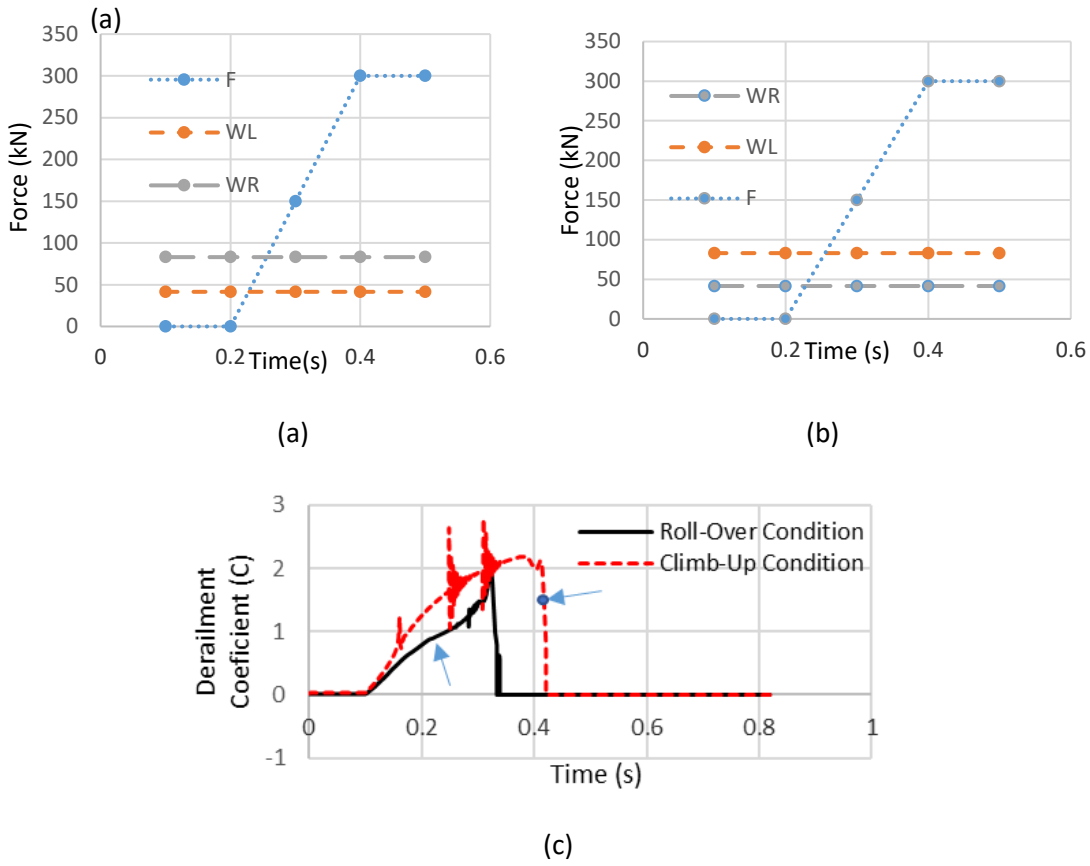

Figure 3. (a) Loading history for assessing the simulation (Roll-over condition). (b) Loading history for assessing the simulation (Climb-up condition). (c) Derailment coefficient of wheelset

shown. The period is 200 milliseconds, and the impact load of 300 kN is applied to the wheelset as a step function in the middle of the time interval. It should be noted that over 90 percent of considered models derail in under 100 milliseconds (derailment response of the wheelset takes less than 100 milliseconds). To obtain the derailment time, the beginning of the impact time is after 100 milliseconds. Then, the changes in the radius of curvature, superelevation, and velocity are examined. In each case, one parameter changes, and the others are considered constant.

2.3. Wheelset model on the curved tracks under a vertical impact due to rail removal

Several reasons such as theft, sabotage, or rail fracture can lead to rail removal. It is shown in Figure 2 (d) that a part of the rail is removed and the length of the removed rail is unlimited, Figure 4 (b) depicts the rail removing function in which there is a sudden drop after 5 meters. The fall of the wheelset due to the lack of rails causes a vertical impact on the wheelset, therefore, in this situation, we are facing a phenomenon that is inherently an impact. This phenomenon till now has not been extensively covered in other studies. So, it is one of the innovative aspects of this work and will be compared with the lateral impact of external force on the wheelset. The purpose of this article is to identify the impact phenomenon in these two cases. By recognizing these phenomena, controlling and minimizing damages to passengers and rail vehicles can be studied.

The specifications of the model for rail removal are as follows; the running velocities are 10, 50, and 90 m/s, the rail type is UIC 60, and the height of wheel drop is 17.2 centimeters.

The rail removal is started 5 meters after the starting point. The radiuses of the curved track are 400, 700, and 1500 meters, and superelevations (Cant) are 0 and 0.15 of a meter. To accurately investigate the wheelset falling, vertical and lateral reactions and lateral deviation of the wheelset are specified.

[DOI: 10.22068/ijrare.306]

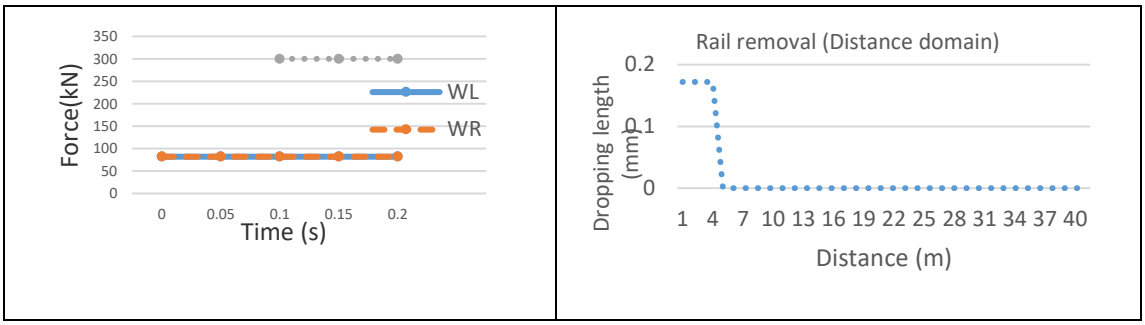

(a) (b)

Figure 4. (a) Loading history for derailment analysis. (b) Distance of rail removal as a step function

3. Results

3.1. Wheelset on straight track (Lateral impact)

A single wheelset on the straight track is used as a criterion for further comparison and analysis. In other words, according to the behavior of the wheelset on a straight path, a better view can obtain regarding the changes in behavior on the curved tracks.

Figure 5 (a) shows the lateral wheelset force reaction for different velocities on a straight track. As the speed of the wheelset increases, the derailment process duration decreases. At the highest velocity (90 m/s), derailment time is reduced by more than 50%, compared to the lowest velocity (25 m/s). As shown in figure 5 (b) at a velocity of 90 m/s the lateral deviation has increased by more than 100% compared to the velocity of 50 m/s. Different results are presented in Tables 2, 3, and 4 considering different speeds, curves, and superelevation.

3.1.1. Wheelset on small radius curves (Lateral impact)

Tables 2, and 3 show the derailment of a single wheelset. The purpose of bringing result is to better understanding of changes and trends.

Two types of derailment exist on a curved track, with differences in the maximum lateral reaction in the wheel and the duration of derailment. Anti-clockwise impact compared to the clockwise impact produces a weaker reaction for each case. Considering the time of the process, the taken time for an anti-clockwise derailment is longer for 60% of cases. We examine changes in velocity, curve radius, and superelevation. It is seen in Tables 2 and 3 that if the speed increases from 25 m/s to 90 m/s for, the taken time for derailment decreases dramatically. At velocities of 75 and 90 meters per second, derailment time is reduced by more than 50%. According to Tables 2 and 3 the maximum lateral reaction force for anti-clockwise derailment mode has reduced by more

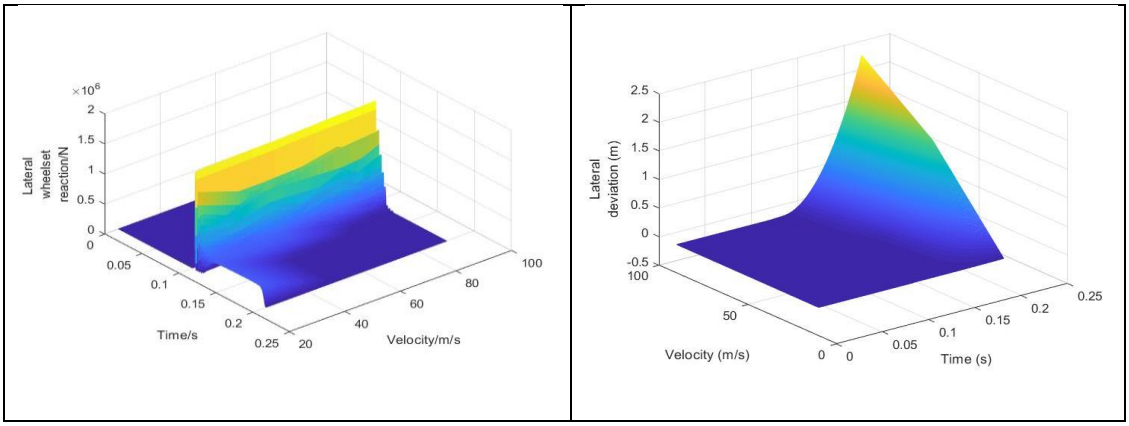

(a) (b)

Figure 5. (a) Lateral wheelset reaction with different velocities on straight track. (b) Lateral deviation of wheelset under lateral impact for different velocities.

[DOI: 10.22068/ijrare.306]

than 100 % on average compared to clockwise derailment mode.

Table 1. Derailment coefficients

	Roll-over Condition	Climb-up condition	The difference for Roll-over Condition (%)	The difference for Climb-up condition (%)
Derailment coefficient (Koo et al) [11] Theoretical	0.9	1.34	4.6	11.9
Derailment coefficient Current model	0.86	1.5	0	0
Derailment coefficient (Koo et al) [11] Simulation	0.96	1.34	6.7	11.9

Table 2. Information of wheelset derailment on small radius curved tracks for different (Cant 0)

Clockwise impact					Anti-clock wise impact				
Speed (m/s)	**Derailment time (ms)**	**Maximum lateral force (kN)**	**Curve (m)**	**Cant (m)**	**Speed (m/s)**	**Derailment time (ms)**	**Maximum lateral force (kN)**	**Curve (m)**	**Cant (m)**
25	88	2800	400	0	25	94	1250	400	0
50	81	2200	400	0	50	41	1900	400	0
75	17	2900	400	0	75	81	800	400	0
90	18	2750	400	0	90	69	1600	400	0
25	84	3200	200	0	25	100	600	200	0
50	30	2800	200	0	50	87	800	200	0
75	26	2750	200	0	75	75	900	200	0
90	15	2750	200	0	90	69	900	200	0
25	73	3250	100	0	25	44	550	100	0
50	61	3200	100	0	50	25	700	100	0
75	63	3000	100	0	75	21	740	100	0
90	64	2900	100	0	90	21	750	100	0
90	64	2900	100	0	90	21	750	100	0

The variations in superelevation do not cause a significant change in the derailment pattern, as seen in Tables 2 and 3, for specific velocity and curve radii there is no noticeable change in the taken time of derailment and maximum wheel lateral reaction force. So, for the same reason, they are not considered for curves with a larger radius.

It has to be noted that for small curves (100, 200, and 400 meters) not much difference is seen between the same modes. For example, considering an anti-clockwise mode or a clockwise mode of derailment, if we change the curve radii and keep the speed and the superelevation constant, the taken time of the derailment and the maximum lateral reaction for the same mode remain nearly constant.

3.1.2. Wheelset on large radius curves (Lateral impact)

Curved tracks are of particular importance because they can create two derailment modes on their own. In curves with large radii of curvature, the derailment patterns resemble those of a straight track. As the curve radii get smaller, the anti-clockwise and clockwise derailment patterns become different from each other. As shown in Table 4 maximum difference between lateral reaction force for anti-clockwise derailment and clockwise derailment is 21 percent and the difference between the time of

[DOI: 10.22068/ijrare.306]

Table 3. Information of wheelset derailment on small radius curved tracks for different (Cant 0.15 m)

Clock wise impact					Anti-clock wise impact			
Speed (m/s)	Derailment time (ms)	Maximum lateral force (kN)	Curve radii (m)	Cant (m)	Speed (m/s)	Derailment time (ms)	Maximum lateral force (kN)	Curve radii (m)
25	88	2750	400	0.15	25	100	1250	400
50	80	2220	400	0.15	50	40	1800	400
75	15	2850	400	0.15	75	81	760	400
90	13	2450	400	0.15	90	71	1600	400
25	81	3120	200	0.15	25	100	600	200
50	32	2800	200	0.15	50	87	800	200
75	26	2750	200	0.15	75	76	920	200
90	18	2750	200	0.15	90	71	900	200
25	72	3150	100	0.15	25	43	600	100
50	63	3150	100	0.15	50	24	600	100
75	63	3000	100	0.15	75	21	700	100
90	66	2850	100	0.15	90	22	750	100

derailment for the two modes is less than 10 percent. According to Table 4 on a curved track with radii of 8000 meters, the difference between derailment time of the clockwise and anti-clockwise modes is less than 20 percent, and the values of maximum lateral reaction for both modes are very close for almost all cases with less than 10% difference.

3.1.3. Differences and similarities of derailment modes due to lateral impact

Due to the similarity and a large number of diagrams, Figure 6 shows four graphs that represent all cases. In Figure 6, the differences and similarities between the two derailment modes in terms of derailment duration and the lateral reaction force of the wheelset are illustrated. In Figure 6 (a), it is understood that although there is not much difference in derailment time, the amplitude of the initial oscillation of the lateral reaction of the wheelset when the derailment is clockwise is five times larger.

According to Figure 6 (b), at the speed of 90 m/s, the pattern of the two derailment modes is very different from each other, both in terms of time and lateral force fluctuations. As seen in Figure 6 (c), at a speed of 25 m/s, the two modes of derailment are very close to each other in terms of the time duration of derailment and oscillation patterns.

From Figure 6 (d), at a speed of 90 m/s and the curve radii of 8000 meters, the patterns of clockwise and anti-clockwise derailment are similar in terms of time duration and amplitudes of the lateral reaction force of the wheelset.

Overall, curve radii have a great influence on the mode of derailment, on small curves, anti-clockwise derailment will occur with the intense reaction, on the other hand, clockwise derailment occurs without intense lateral reaction and takes a longer time.

3.1.4. The lateral impact force, causing the derailment on the curved track

Until now, all lateral forces were considered equal to 300 kN. But in this part, the goal is to obtain the force that causes derailment on the curved tracks. In Figures 7 (a) and 7 (b), the axis corresponding to the size of the curve radii is given logarithmically. In Figure 7 (a), the data scatter seems to be high. But in Figure 7 (b), the trend seems to be more pronounced. From figure 7(a) we can realize that the derailing force is not considerably affected by curve radii and velocity. According to Figure 7 (b) for anti-clockwise derailment as the velocity increases the derailing force decreases and curve radii has not a considerable effect on derailing force. The average forces that cause derailment in the clockwise and anti-clockwise modes are 245 kN and 213 kN, respectively. The difference is 13 percent; it can be realized that ant- clockwise derailment is relatively easier to occur.

3.2. Wheelset on the curved tracks having vertical impact due to rail removal

In this section important parameters are the velocity of the wheelset, and the removal of the inner rail or outer rail. According to Table 5, the behavior of the wheelset on different curves considering the rail removal is similar. When the

[DOI: 10.22068/ijrare.306]

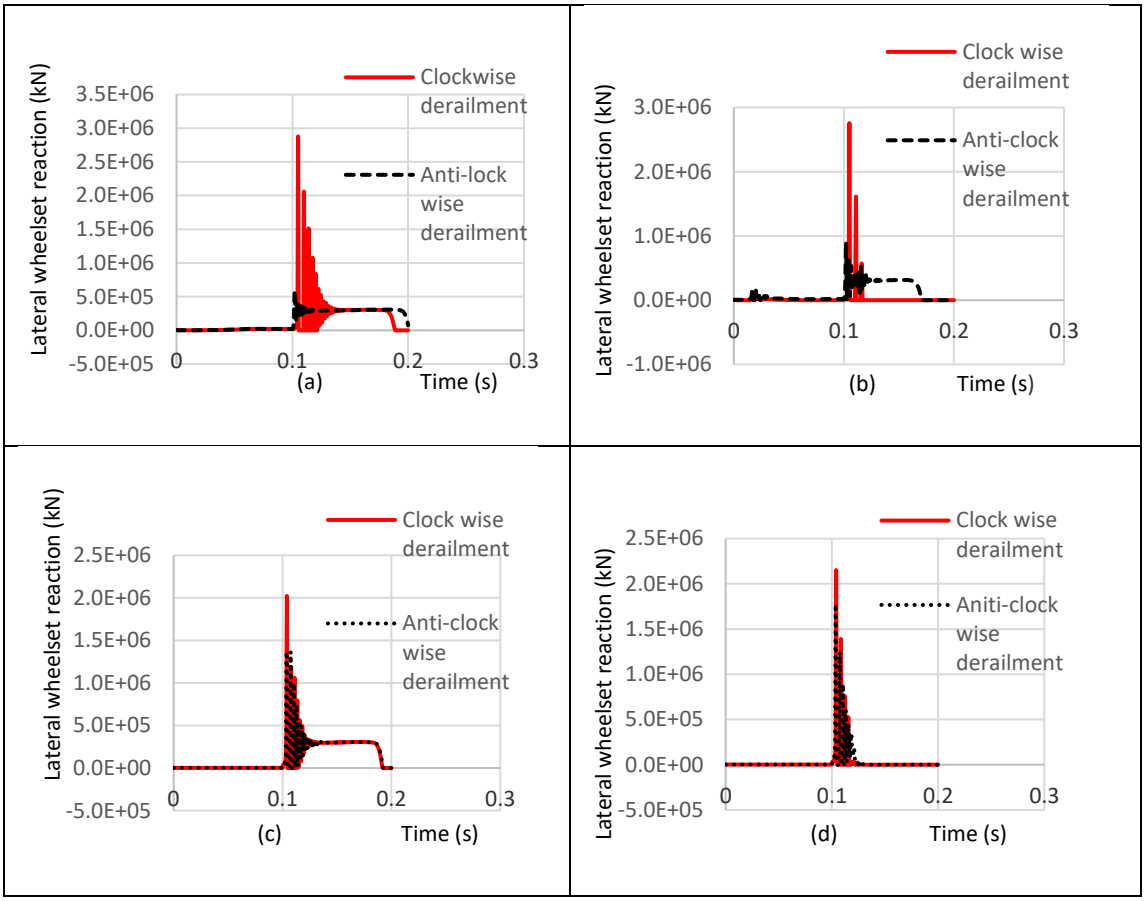

Figure 6. (a) Derailment of clockwise and anti-clock wise mode (Velocity 25 m/s, curve radii 200 m). (b) (Velocity 90 m/s, curve radii 200 m). (c) (Velocity 25 m/s, curve radii 8000 m). (d) (Velocity 90 m/s, curve radii 8000 m)

outer rail (the rail is farther from the center of the curve) is removed considering higher velocities (above 40 m/s), derailment always occurs.

Considering outer rail removal, the higher the speed, the greater the lateral deviation of the wheelset. At a speed of 90 m/s, lateral deviation increases, and at the derailment moment, it is unlimited. In the case of the inner rail removal considering the velocities even above 50 m/s, no derailment will occur. For the cases of the inner rail removal, after the wheelset falls, there is a limited lateral deviation before returning to a stable condition (no derailment) therefore their diagrams were not taken into account. Vertical and lateral force reactions have to be considered in case of derailment due to rail removal. Vertical and lateral forces divide by the weight of the wheelset (166 kN) to obtain the normalized values.

Due to the wheelset falling, a strong vertical impact and lateral reaction will be produced. In this part, the lateral reaction is a function of vertical force, around a third of the vertical reaction. Besides, in the absence of lateral impact. Different superelevations do not have a tangible effect on vertical and lateral wheelset reactions and lateral deviation of the wheelset. Since the time duration of vertical forces is very short, the sampling times in Figures 8-10 must be small enough to cover these impacts after the wheelset falls.

From Table 5, the differences in maximum vertical reaction forces are less than 5% for different curve radii, different superelevation, different velocities, and rail removal conditions. Table 5 shows that in the case of the inner rail removal, the derailment does not occur even at velocities higher than 50 m/s. However, if the outer rail is removed, the wheelset will be derailed at velocities around 50 m/s. Similar patterns are obtained for different curve radii for derailment due to removing the rail. The main reason for derailment, when the outer rail is removed is loss of resistance to centrifugal force, with the increase in velocity the centrifugal force increases as well. As shown For the cases with outer rail removal when the velocity reaches

[DOI: 10.22068/ijrare.306]

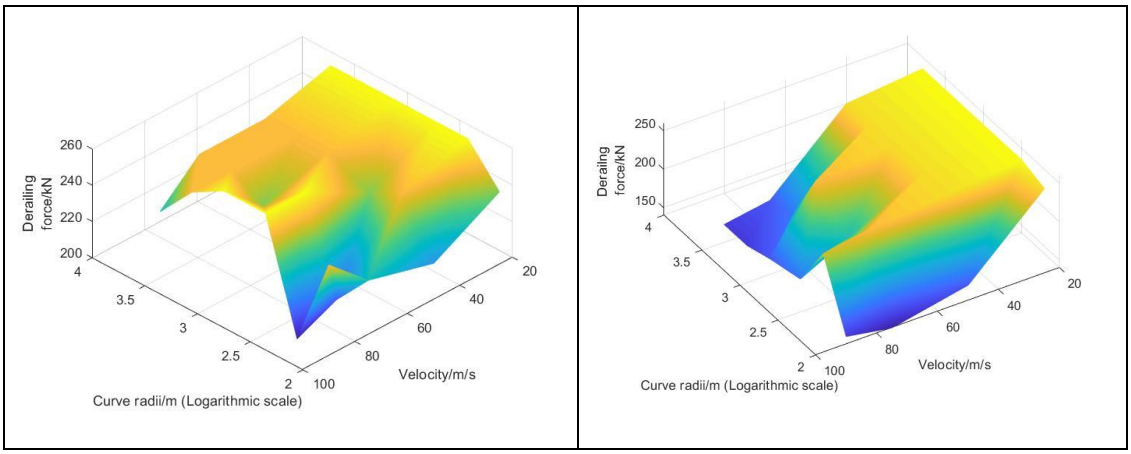

Figure 7. (a) Derailing force (Clockwise Derailment). (b) Derailing force (Anti-clockwise Derailment)

around 50 m/s lateral deviation increases substantially which is considerably higher compared to cases with lower velocity (10 m/s) in these cases (50 m/s or 90 m/s) derailment occurs.

Since there are too many diagrams and they are very similar only the diagrams related to curve radii of 400 meters are presented. Figures 8, 9, and 10 relating to vertical force, lateral force, and lateral deviation of the wheelset on the 400-meter curve (outer rail removal condition) are presented.

As can be seen in Figures 8 (a), 9 (a), and 10 (a), vertical reaction forces for two superelevations (0 and 0.15 m) are plotted, considering both left and right wheels. A vertical reaction appears in a very short time with a significantly large value. Considering the speed of 10 m/s, after the first impact, the vertical forces will be damped, and no significant force arises on the side where the wheel is not fallen. Superelevations do not affect the pattern and values of the vertical reaction forces.

Figures 8 (b), 9 (b), and 10 (b) depict the lateral reaction force of the right wheel and left wheel for two superelevations. The negative sign of lateral forces is related to the direction of the force. The falling wheel has a remarkable lateral force compared to the stable wheel. The maximum lateral force of the stable wheel is 10% of that of the falling wheel. After falling, with a velocity of 10, significant lateral force appears. At the velocities of 50 m/s and 90 m/s, the same pattern is seen and lateral forces will arise.

Figures 8 (c), 9 (c), and 10 (c) show the lateral deviation of wheels. At a velocity of 10 m/s, from Figure 8 (c), it is seen that there is sudden lateral deviation and then returning to a stable condition. As the velocity increases to 50 m/s, a substantial lateral deviation occurs that exceeds 30 cm and changes its direction at the end of the analysis stage, and derailment will occur. When the velocity reaches 90 m/s after falling off the wheel, the lateral deviation of the wheels becomes very large (unlimited), and the wheelset derails as if there is a lateral impact.

As mentioned before if the velocity increases the centrifugal force increases and lateral deviation increases as well. By removing the inner rail derailment will not occur since there is a barrier against the centrifugal force but if the outer rail is removed derailment will occur.

3.3. Comparison of wheelset under lateral external impact and falling due to rail removing

In the case of the lateral impact, it is noteworthy that there is more lateral reaction than vertical reaction. Under the influence of the lateral force, the flange area of the wheel hits the rail and causes a large reaction. While the other wheel has much less lateral force, and eventually, the vertical reaction of the wheelset is less than the lateral reaction, which leads to derailment. In the case of rail removal, a strong vertical force is created immediately. Due to the nature of the impact, the vertical reaction is very intense. Since we do not have a lateral impact, in this case, the lateral reaction resulting from a vertical impact is less than the vertical force reaction (about 60% less) and is affected by the friction coefficient, therefore, in this case, the lateral force, which is less than the vertical force, cannot cause a derailment, and high centrifugal force due to the velocity leads to the derailment.

[DOI: 10.22068/ijrare.306]

Table 4. Information of wheelset on the 400-meter, 700-meter and 1500-meter curve

Maximum normalized vertical reaction force	Maximum normalized lateral reaction force	Lateral deviation after falling (mm)	Curve radii (m)	Cant (m)	Inner or outer rail removing condition	Velocity (m/s)	Derailment status
79.27	28.96	32.5	400	0	Inner	10	no
79.27	28.96	33	400	0	Inner	50	no
79.27	27.44	32	400	0	inner	90	no
79.27	28.96	32.5	400	0	outer	10	no
79.27	28.96	200	400	0	outer	50	yes
76.22	25.61	Infinite	400	0	outer	90	yes
79.27	28.96	32.5	400	0.15	inner	10	no
79.27	28.05	34	400	0.15	inner	50	no
76.22	27.44	32.5	400	0.15	inner	90	no
79.27	28.96	32.5	400	0.15	outer	10	no
79.27	28.96	200	400	0.15	outer	50	yes
76.22	25.91	Infinite	400	0.15	outer	90	yes
79.27	28.96	32.5	700	0	inner	10	no
79.27	28.96	35	700	0	inner	50	no
76.22	25.91	27	700	0	inner	90	no
79.27	28.96	32.5	700	0	outer	10	no
79.27	27.44	170	700	0	outer	50	yes
73.17	23.17	Infinite	700	0	outer	90	yes
79.27	28.96	32.5	700	0.15	inner	10	no
79.27	28.96	35	700	0.15	inner	50	no
79.27	28.96	22	700	0.15	inner	90	no
79.27	28.96	32	700	0.15	outer	10	no
79.27	28.05	170	700	0.15	outer	50	yes
73.17	23.17	Infinite	700	0.15	outer	90	yes
79.27	28.96	32.5	1500	0	inner	10	no
79.27	28.96	37	1500	0	inner	50	no
79.27	26.22	30	1500	0	inner	90	no
79.27	28.96	32.5	1500	0	outer	10	no
79.27	28.96	50	1500	0	outer	50	yes
73.17	23.17	Infinite	1500	0	outer	90	yes
79.27	28.96	32.5	1500	0.15	inner	10	no
79.27	27.44	37	1500	0.15	inner	50	no
79.27	27.44	30	1500	0.15	inner	90	no
79.27	28.96	32.5	1500	0.15	outer	10	no
79.27	25.91	170	1500	0.15	outer	50	yes
73.17	23.17	Infinite	1500	0.15	outer	90	yes

Figure 5 (b) shows the lateral deviation of the wheelset under a lateral impact. As the velocity increases, the lateral deviation increases dramatically, at velocities near 90 m/s on the curves, wheelset derailment due to the rail removing has an infinite lateral deviation similar to the derailment due to the lateral impact.

3.4. Final remarks and suggestions

The lateral energy absorber can be used in both cases since the lateral sides of rail vehicles undergo strong lateral impact for the lateral impact case and overturning for rail removing condition. According to data on lateral impact force in the previous part for the lateral impact, the derailing force is almost between 90 percent to 150 percent of the wheelset weight and its loads (166 kN). According to table 5, the vertical impact force is almost 80 times bigger than the weight of the single wheelset and its loads (166 kN).

[DOI: 10.22068/ijrare.306]

From Figures 7 (a) and 7 (b) the minimum and maximum derailing force are around 150 kN and 250 kN respectively, the lateral impact absorber can be located on the lateral sides of the rail vehicle in case of a possible lateral crash and transfer smaller lateral force to the vehicle.

Although, the vertical reaction force caused by rail removal is very intensive and large without high velocity and centrifugal forces derailment will not take place. Velocity, the centrifugal force of the rail vehicle, and side of the rail removing on the curve track plays the most important role in this derailment process. Energy absorbers or passive safety systems can be utilized with primary and secondary suspensions to minimize the effect of vertical impact and its damage to passengers and rail vehicles.

4. Conclusions

4.1. Derailment due to lateral impact

•As the speed increases, the derailment process time decreases. Small curves can intensify this effect.

•The difference in superelevations does not cause such changes in the time and the pattern of derailment.

•Anti-clockwise derailment can occur more easily.

•Smaller force (below 200 kN) is required to derail the wheelset at high speeds.

•Most important of all is the effect of the curve on the derailment pattern. In sharp curves, there are two patterns of derailment. If the impact is toward the inside of the curves, a strong lateral reaction force is created by the

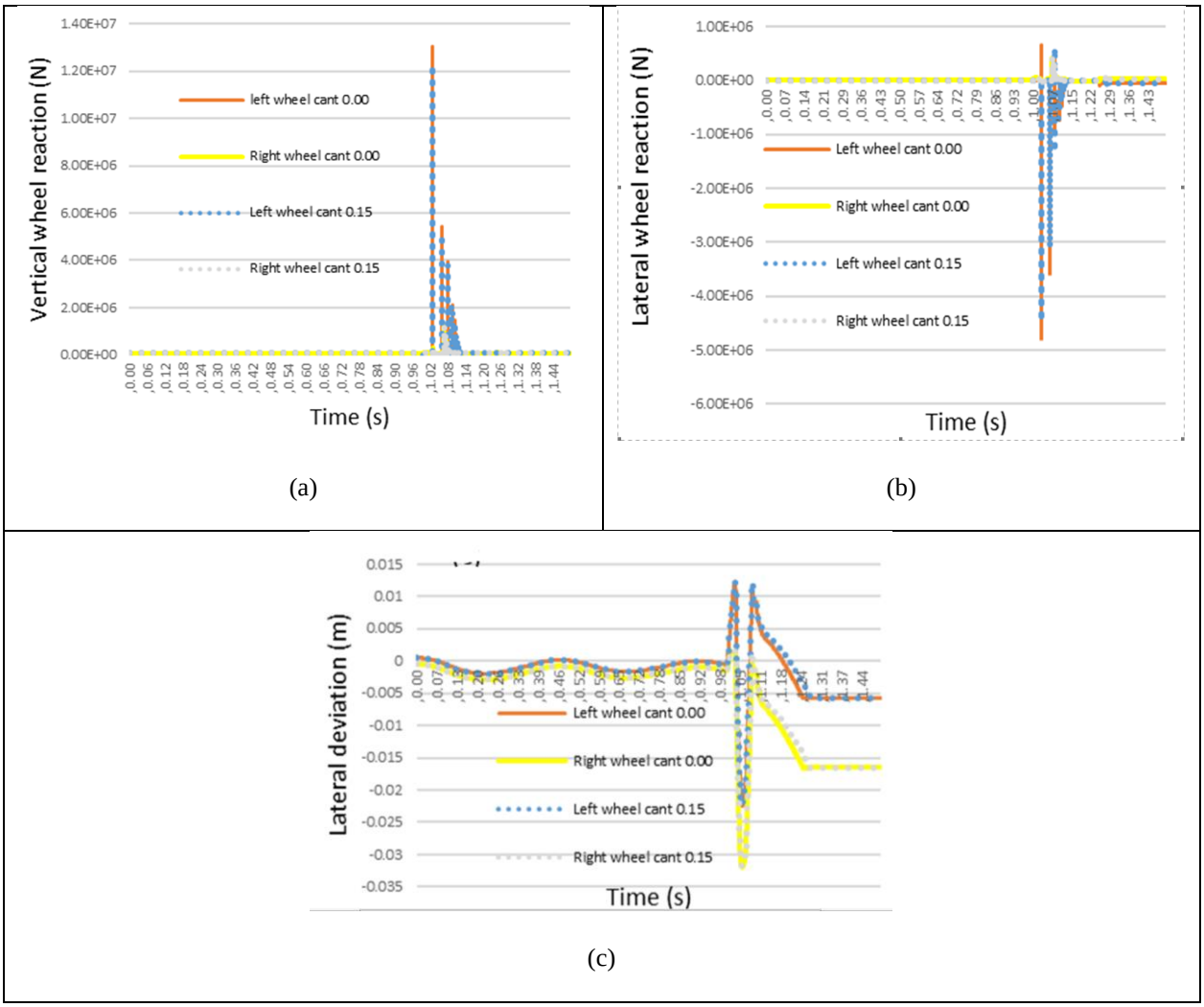

Figure 8. (a) Vertical wheel force (10 m/s), (b) Lateral wheel force (10 m/s), (c) Lateral deviation of wheels (10 m/s)

[DOI: 10.22068/ijrare.306]

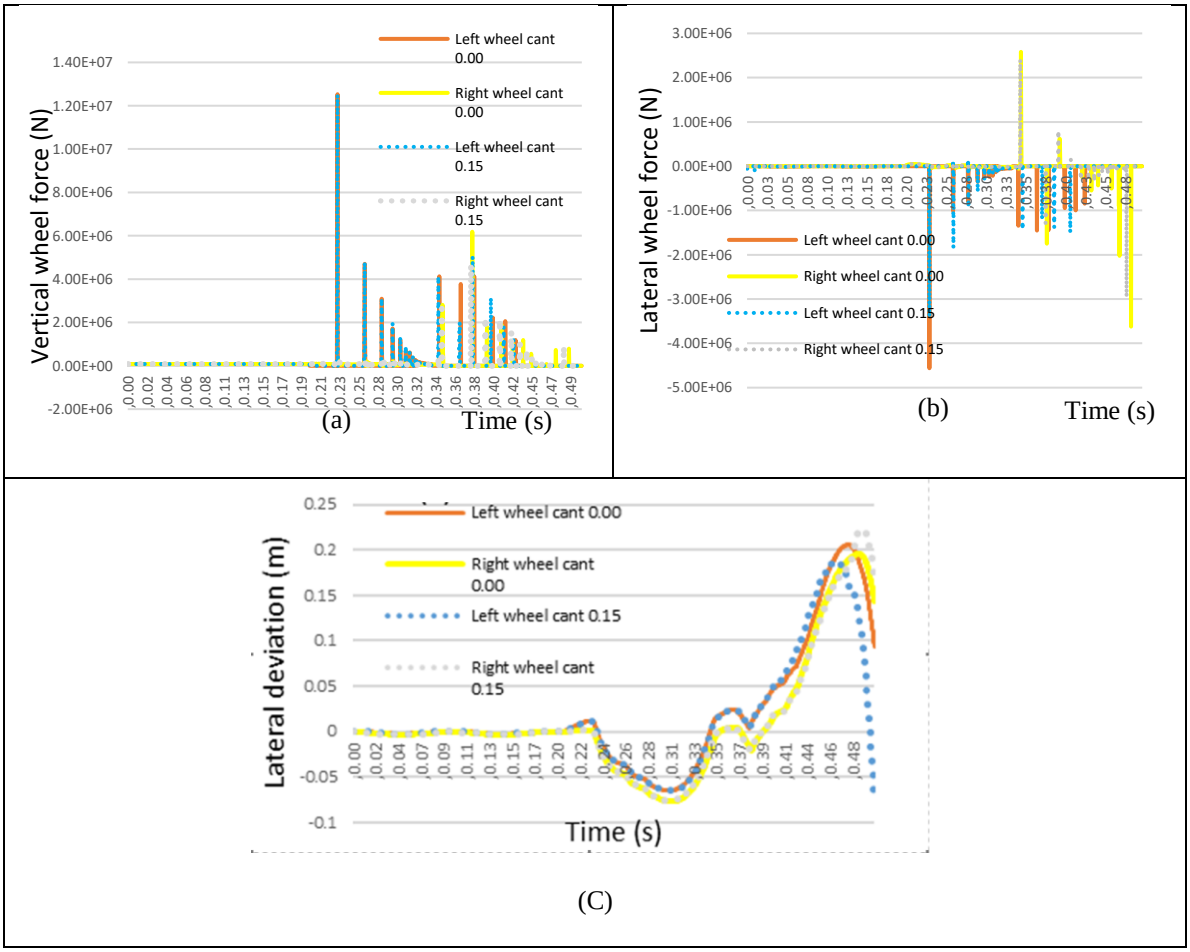

Figure 9. (a) Vertical wheel force (50 m/s). (b) Lateral wheel force (50 m/s). (c) lateral deviation of wheels (50 m/s)

wheelset. So, derailment is accompanied by severe fluctuations in lateral reaction force.

•In curves where the radius of curvature is large enough, the clockwise and anti-clockwise

derailment patterns are very similar to each other in terms of derailment time and lateral reaction force fluctuation.

4.2. Derailment due to rail removal

• In the case of vertical impact as a result of the rail removal, the lateral reaction of the wheelset is a function of the vertical force.

•When the outer rail is removed there will be a loss of resistance to centrifugal force.

•At a velocity of 50 m/s, derailment due to the outer rail removal happens under any condition on the curved tracks. However, at a velocity of 10 m/s, the lateral deviation is limited for all curves. As the velocity increases from 50 m/s to 90 m/s, the lateral deviation approaches unlimited value.

•At the velocity of 90 m/s, the derailment pattern due to rail removing is similar to that of the wheelset under the lateral impact.

•When the wheelset touches the ground for the first time, a vertical reaction force appears. This force is 80 times greater than the weight of the wheelset. If the inner rail is removed in the curved track, derailment will not occur under any circumstances.

•It is possible to design crash energy absorbers and passive safety systems considering the derived reaction impact forces.

[DOI: 10.22068/ijrare.306]

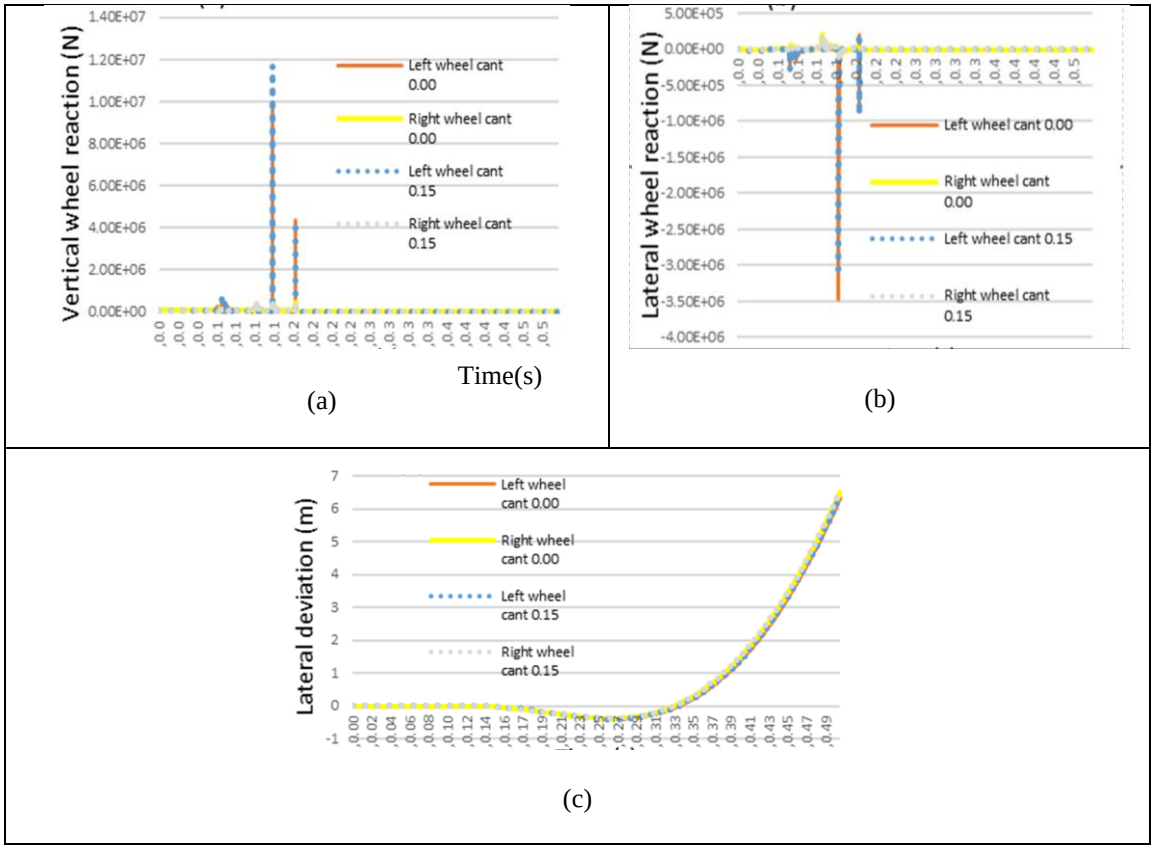

Figure 10. (a) Vertical wheel force (90 m/s). (b) Lateral deviations of wheels (90 m/s) .(c) Lateral wheel force (90 m/s)

[DOI: 10.22068/ijrare.306]

References

[1] Pater, A, The General Theory of the Motion of a Single Wheelset Moving through a Curve with Constant Radius and Cant, Journal Of Applied Mathematics And Mechanics, ZAMM.61, 277-293, (1981).

[2] Iwincki S, Simulation of Wheel-rail contact force, Fatigue and Fracture of Engineering Materials & Structures, 26, 887-900, (2003).

[3] Xiang J, Zeng Q, Lou P, Theory of random energy for train derailment, Journal of Central South University of Technology, 1005 - 9784 02- 0134- 06, (2003).

[4] Sweet L, Karmel A, Moy P, Wheelset Derailment Criteria Under Steady Rolling and Lateral Impact Conditions, Vehicle System Dynamics, 8:2-3, 229-234, (2007).

[5] Kim S, Kwon T, Koo J, Crashworthiness Evaluation of the Korean High Speed Train Using a Virtual Testing Model, International Journal of Modern Physics B, Vol. 22, No. 09n11, 1383-1390, (2008).

[6] Koo J, Cho S, A method to predict the derailment of rolling stock due to collision using a theoretical wheelset derailment model, Multibody System Dynamics, 27: 403-422, (2011).

[7] Torstensson P, Nielsen J, Simulation of dynamic vehicle–track interaction on small radius curves, Vehicle System Dynamics: International Journal of Vehicle Mechanics and Mobility, 49:11, 1711-1732, (2011).

[8] Koo J, Choi S, Theoretical development of a simplified wheelset model to evaluate collision-induced derailments of rolling stock, Journal of Sound and Vibration, 331: 3172-3198, (2012).

[9] Zhou H, Wang B, Hecht M, Three-dimensional derailment analysis of a crashed city tram, Vol. 51, No. 8, 1200-1215, (2013).

[10] Cases J, Gialleonardo E, Bruni S, Baeza L, A comprehensive model of the railway wheelset–track interaction in curves, Journal of Sound and Vibration, 333: 4152-4169, (2014).

[11] Koo J, Oh H, A new derailment coefficient considering dynamic and geometrical effects of a single wheelset, Journal of Mechanical Science and Technology, 28 (9): 3483-3498, (2014).

[12] Liu P, Wang K, Effect of braking operation on wheel–rail dynamic interaction of wagons in sharp curve, Journal of Multi-Body Dynamics 231(1) 252-265, (2016).

[13] Ling L, Dhanasekar M, Thambiratnam D,Sun Y, Lateral impact derailment mechanisms, simulation and analysis, International Journal of Impact Engineering, Volume 94,Pages 36-49, (2016).

[14] Ling L, Dhanasekar M, Thambiratnam D, Frontal collision of trains onto obliquely stuck road trucks at level crossings: Derailment mechanism and simulation, International Journal of Impact Engineering, 100: 154-165, (2016).

[15] Ling L, Dhanasekar M, Thambiratnam D, Minimizing lateral impact derailment potential at level crossings through guard rails, International Journal of Mechanical Sciences, 113: 49-60, (2016).

[16] Ling L, Dhanasekar M, Thambiratnam D, Assessment of road-rail crossing collision derailments on curved tracks, Australian Journal of Structural Engineering, 18:2, 125-134, (2017).

[17] Ling L, Dhanasekar M, Thambiratnam, Dynamic response of the train–track–bridge system subjected to derailment impacts, Vehicle System Dynamics, (2017).

[18] Yao S, Zhu H, Yan K, Liu M, Xu P, The derailment behavior and mechanism of a subway train under frontal oblique collisions, Internation Journal of Crashworthiness, (2019).

[19] Ling L, Dhanasekar M, Wang K, Zhai W, Weston B, Collision derailments on bridges containing ballastless slab tracks, Engineering Failure Analysis, 105: 869-882, (2019).

[20] Yao S, Zhu H, Liu M, Li Z, Xu P, Che Q, A study on the frontal oblique collision-induced derailment mechanism in subway vehicles, Journal of Rail and Rapid Transit, 0(0) 1-12, (2019).

[21] Gao G J, Zhou T Y, Guan W Y, Recent research development of energy-absorption structure and application for railway vehicles, Journal of Central South University of Technology, 27: 1012-1038, (2020).

[22] Choi I, Um J, Lee J, Choi H, The influence of track irregularities on the running behavior of high-speed trains, Journal of Rail and Rapid Transit, 227 (1) 94-102, (2012).

[23] Cheng Y, Hsu T, Derailment safety analysis for a tilting railway vehicle moving on irregular

[DOI: 10.22068/ijrare.306]

tracks shaken by an earthquake, Journal of Rail and Rapid Transit, 0(0) 1-18, (2014).

[24] Dyk B, Edwards J, Dersch M, Rupert Jr C, Barkan C, Evaluation of dynamic and impact wheel load factors and their application in design processes, Journal of Rail and Rapid Transit, 0(0) 1–11, (2016).

[25] Cheng C, Chen C, Hsu C, Derailment and Dynamic Analysis of Tilting Railway Vehicles Moving Over Irregular Tracks Under Environment Forces, International Journal of Structural Stability and Dynamics, Vol. 17, No. 9, (2017).

[DOI: 10.22068/ijrare.306]